Neuron, Vol. 45, 847–859, March 24, 2005, Copyright ©2005 by Elsevier Inc. DOI 10.1016/j.neuron.2005.01.032

Mouse Model of Multiple System Atrophy α-Synuclein Expression in Oligodendrocytes Causes Glial and Neuronal Degeneration

Ikuru Yazawa,[1] Benoit I. Giasson,[2] Ryogen Sasaki,[1] Bin Zhang,[1] Sonali Joyce,[1] Kunihiro Uryu,[1] John Q. Trojanowski,[1,3] and Virginia M.-Y. Lee[1,3,*]
[1]Center for Neurodegenerative Disease Research
Department of Pathology and Laboratory Medicine
[2]Department of Pharmacology
[3]Institute on Aging
University of Pennsylvania School of Medicine
Philadelphia, Pennsylvania 19104

Summary

Transgenic (Tg) mice overexpressing human wild-type α-synuclein in oligodendrocytes under the control of the 2′, 3′-cyclic nucleotide 3′-phosphodiesterase (CNP) promoter are shown here to recapitulate features of multiple system atrophy (MSA), including the accumulation of filamentous human α-synuclein aggregates in oligodendrocytes linked to their degeneration and autophagocytosis of myelin. Significantly, endogenous mouse α-synuclein also accumulated in normal and degenerating axons and axon terminals in association with oligodendroglia and neuron loss and slowly progressive motor impairments. Our studies demonstrate that overexpression of α-synuclein in oligodendrocytes of mice results in MSA-like degeneration in the CNS and that α-synuclein inclusions in oligodendrocytes participate in the degeneration of neurons in MSA.

Introduction

Growing evidence suggests that nonneuronal cells play a role in neurodegenerative diseases. For example, activated microglia associated with amyloid deposits in Alzheimer's disease (AD) may contribute to brain degeneration (Perlmutter et al., 1990; McGeer et al., 1993), and nonneuronal cells modulate the survival of motor neurons expressing mutant SOD1 in amyotrophic lateral sclerosis (ALS) transgenic (Tg) mouse models (Clement et al., 2003). Astrocytes also can propagate prion infectivity in Tg mice, where the hamster prion protein (PrP) is expressed using the glial fibrillary acidic protein (GFAP) promoter (Raeber et al., 1997).

Multiple system atrophy (MSA) is a neurodegenerative disease that affects oligodendrocytes and neurons in the human central nervous system (CNS). MSA is a sporadic synucleinopathy that is characterized by abnormal accumulations of filamentous α-synuclein inclusions in the CNS (Spillantini and Goedert, 2000; Duda et al., 2000a; Duda et al., 2000b). These α-synuclein inclusions, though present in the cytoplasm and nucleus of neurons, are most prominent in oligodendrocytes, where they are known as glial cytoplasmic inclusions (GCIs), and GCIs are diagnostic of MSA (Papp et al., 1989; Arima et al., 1998; Spillantini et al., 1998; Tu et al., 1998). Clinically, MSA presents with Parkinsonism, ataxia, and autonomic failure (Graham and Oppenheimer, 1969). Previously, MSA was thought to be three separate diseases known as striatonigral degeneration, olivopontocerebellar atrophy (OPCA), and Shy-Drager syndrome, but with recognition that GCIs are the defining lesions in all three diseases, the classification of patients with MSA has been simplified to MSA-C (cerebellar ataxia) or MSA-P (parkinsonism), depending on the relative predominance of clinical and pathological abnormalities (Gilman et al., 1999).

Although mechanisms of neurodegeneration in MSA are unclear, we hypothesize that oligodendrocytic degeneration is a consequence of α-synuclein inclusions and that GCIs contribute significantly to neuronal degeneration in MSA. Since accumulations of human wild-type α-synuclein in neurons led to the formation of neuronal α-synuclein aggregates and dopaminergic degeneration in a mouse model of Parkinson's disease (Masliah et al., 2000), accumulation of α-synuclein in CNS oligodendrocytes may be linked to mechanism(s) underlying MSA. To examine this possibility, we have generated a Tg mouse model that expresses human wild-type α-synuclein in oligodendrocytes of the mouse CNS (Giasson et al., 2003) under the control of the 2′, 3′-cyclic nucleotide 3′-phosphodiesterase (CNP) promoter (Gravel et al., 1998). Since oligodendrocytes in the Tg mice developed age-dependent accumulations of human α-synuclein into GCIs concomitant with brain degeneration, we asked if oligodendrocytic degeneration also causes neuronal degeneration. Here, we demonstrate that the formation of GCI-like α-synuclein inclusions leads directly to neuronal degeneration as exemplified by motor impairments and novel accumulations of endogenous mouse α-synuclein in the brain and spinal cord. The motor impairments were associated with the degeneration of oligodendrocytes and axons in the CNS, indicating that the Tg mice developed a neurodegenerative synucleinopathy with close verisimilitude to authentic MSA. Thus, our study shows that the accumulation of α-synuclein as GCIs can lead to neurodegeneration in Tg mice, and we suggest that similar processes underlie MSA.

Results

Generation of Tg Mice Expressing Human Wild-Type α-Synuclein in Oligodendrocytes

The murine CNP promoter was used to drive expression of human α-synuclein in oligodendrocytes of Tg mice (M2 mice) (see Figure 1A) (Gravel et al., 1998). Immunoblotting analysis with antibodies against human α-synuclein demonstrated the expression of this transgene in the brain of M2 mice (Figure 1B). Since endogenous α-synuclein is predominantly found in neurons with very low levels expressed in oligodendrocytes, it was not possible to determine the level of human α-synuclein overexpression in oligodendrocytes in our Tg mice. However, the overall human α-synuclein

*Correspondence: vmylee@mail.med.upenn.edu

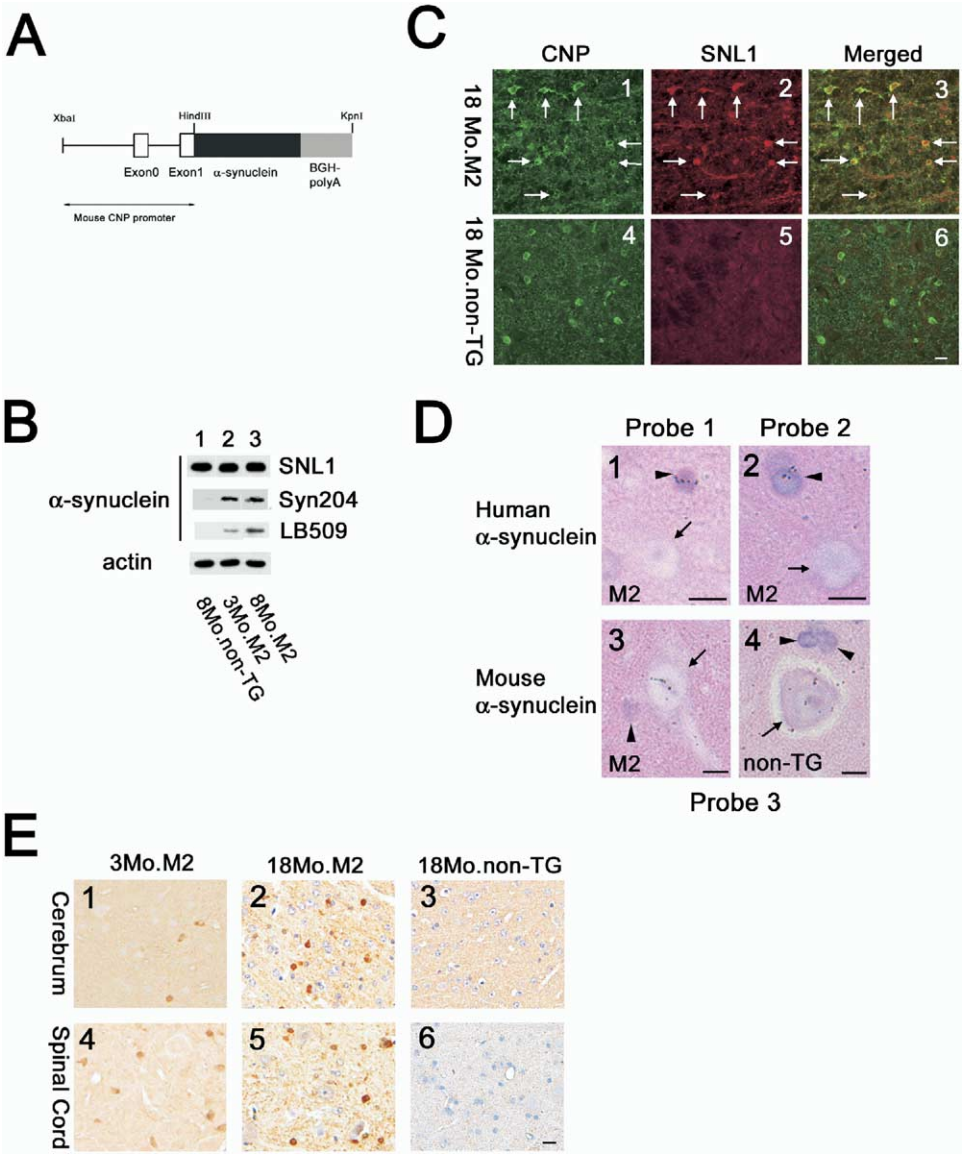

Figure 1. Expression of Human α-Synuclein in M2 Mice

(A) Schematic representation of the cDNA construct used to generate Tg mice expressing human α-synuclein in CNS oligodendrocytes under the control of the murine CNP promoter.

(B) Immunoblotting analysis of α-synuclein expression in an 8-month-old non-Tg mouse (lane 1; 8 Mo. non-Tg), a 3-month-old M2 mouse (lane 2; 3 Mo. M2), and an 8-month-old M2 mouse (lane 3; 8 Mo. M2). Total protein brain homogenates were separated on SDS-PAGE gels, and blots were analyzed with three anti-α-synuclein antibodies (Syn204, LB509, and SNL1). SNL1 detects both murine and human α-synuclein; Syn204 selectively recognizes human α-synuclein; and LB509 is specific for human α-synuclein. Immunoblotting for actin was used as a loading control.

(C) Double-label immunofluorescence staining of white matter of the spinal cord in 18-month-old M2 (C1–C3) and age-matched nontransgenic (C4–C6) mice. CNP colocalizes with α-synuclein (SNL1) in the cytoplasm of the oligodendrocytes in M2 mice (arrows). Scale bar, 15 μm.

(D) In situ hybridization was used to assess the expression of α-synuclein mRNA in 12-month-old M2 and age-matched non-Tg mice. Micrographs of emulsion-dipped in situ hybridization with two probes specific for human α-synuclein mRNA show that human α-synuclein is expressed only in oligodendrocytes (arrowheads), but not in neurons (arrows) (D1 and D2). In contrast, the in situ hybridization using a probe specific for mouse endogenous α-synuclein mRNA reveals that mouse α-synuclein is expressed in neurons (arrows), but not in oligodendrocytes (arrowheads), in the M2 Tg (D3) and in non-Tg control mice (D4). Scale bar, 6 μm.

(E) Immunohistochemical analysis of cerebral cortex (cerebrum) and spinal cord in 3-month-old M2 (E1 and E4) and 18-month-old M2 Tg mice (E2 and E5), and age-matched controls (E3 and E6). SNL1 staining shows the typical neuropil distribution of α-synuclein in addition to α-synuclein expression in oligodendrocytes of M2 Tg mice, but not in oligodendrocytes of non-Tg mice. No pathological change is observed in the neuropil of M2 Tg mice at 3 months, but accumulations of α-synuclein are detected in the neuropil at 18 months. Scale bar, 15 μm.

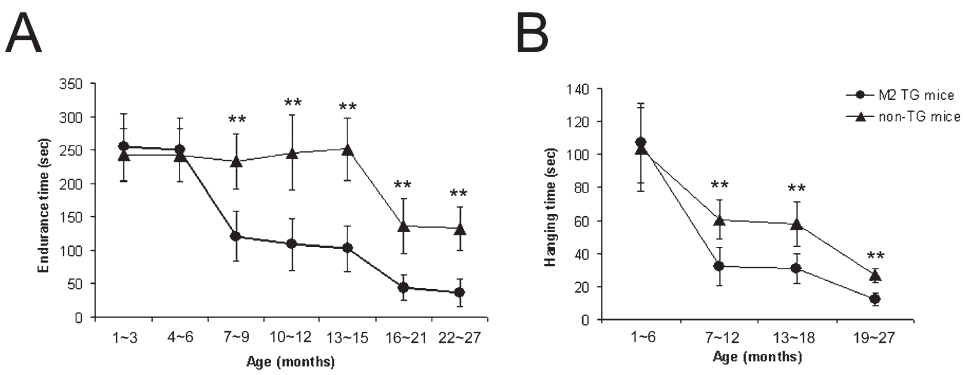

Figure 2. Motor Impairment in M2 Mice

(A) Rotarod treadmill test documenting impaired motor performance in M2 Tg mice compared to non-Tg mice. Motor impairment in M2 mice starts between the ages of 7 and 9 months. Error bars show the standard error of the means. **p < 0.01, Student's t test.
(B) Wire hanging test demonstrating impaired motor ability in M2 mice by 7 months of age (**p < 0.01).

overexpression in oligodendrocytes was relatively low, since the levels of total α-synuclein (both human and endogenous mouse) expression as detected by SNL1 did not differ significantly between non-Tg and the M2 Tg line (Figure 1B). Northern analysis of Tg human and endogenous mouse α-synuclein mRNA in M2 and non-Tg mouse brain indicated that the levels of human α-synuclein mRNA were much less than those of endogenous mouse α-synuclein in M2 Tg mice (Figure S1). Nevertheless, we observed an age-dependent increase in human α-synuclein in total brain homogenates from the M2 mice, suggesting an accumulation of α-synuclein protein in oligodendrocytes as the animals aged. To demonstrate that the cells expressing human α-synuclein were indeed oligodendrocytes in M2 mice, double-label immunofluorescence staining was conducted with anti-α-synuclein and anti-CNP (a marker of oligodendrocytes) antibodies. The colocalization of human α-synuclein with CNP confirmed that oligodendrocytes are the only cells that express human α-synuclein (Figure 1C). In situ hybridization with two human α-synuclein-specific probes revealed the selective presence of human α-synuclein mRNA in oligodendrocytes but not in neurons of M2 mice (Figure 1D). The distribution of human α-synuclein in oligodendrocytes was analyzed next by immunohistochemistry in brain and spinal cord of 3-, 10-, 18-, and 24-month-old M2 mice, and we demonstrated that α-synuclein also accumulated in the neuropil with increasing age (Figure 1E2 and 1E5).

CNP-α-Synuclein M2 Mice Develop Age-Related Motor Impairments and Neurodegeneration

To assess if the expression and progressive accumulation of human α-synuclein in oligodendrocytes give rise to a clinical phenotype, we examined the motor function of M2 mice. Tg mice did not exhibit any motor impairment on a flat surface except for slow motor activity when compared with non-Tg mice. However, when M2 mice were subjected to other motor testing paradigms, they showed several distinct motor impairments when compared with age-matched non-Tg mice (Figures 2A and 2B). For example, the rotarod treadmill test revealed a decrease in the endurance time for motor performance beginning at 7–9 months of age (Figure 2A). However, the weekly rotarod test in mice examined from 6 weeks to 32 weeks showed no significant difference between M2 and non-Tg mice (data not shown), consistent with an age-related rather than a developmental motor abnormality in M2 mice. To assess pure muscle strength of mouse forepaws, the mice were examined in a wire hanging test. This test confirmed a progressive reduction in grip strength of M2 mice with advancing age (Figure 2B), and this was associated with progressive brain atrophy (Figure 3A). Quantitative analysis of brain weight in M2 (n = 5) and control non-Tg (n = 5) mice demonstrated a 16% reduction at 24 months of age (p < 0.01) and an 8.8% decrease at 9 months of age (p < 0.01) in M2 mice (Figure 3B). There was no significant change in brain weight between M2 and non-Tg mice at 1 and 3 months of age, thereby indicating no developmental abnormality in M2 mice. The brain atrophy reflected a reduction in the neuropil and white matter, which most likely resulted from cell loss in M2 mice (Figure 3C). Despite this reduction in brain size, the life span of M2 mice was not affected compared with non-Tg mice. At the age of 24 months, the survival rate was 89% in M2 mice (n = 36) and 83% in control non-Tg mice (n = 30). The longest survival span was 33 months in M2 mice and 34 months in controls.

To assess if the motor impairments are associated with oligodendrocytic and/or neuronal degeneration in M2 mice, quantitative analyses of oligodendrocytes and neurons in the spinal cord were performed in 24-month-old M2 Tg and age-matched non-Tg control mice. These analyses showed a decrease in the number of oligodendrocytes and neurons in the M2 mice compared to the non-Tg mice (Figure 3E). In particular, neuronal loss was most prominent in the lateral and medial columns of M2 mice (Figure 3D). Quantitative analyses of dopaminergic neurons, however, showed no decrease in M2 mice (data not shown).

Pathological Changes in the CNS of M2 Mice

Since human α-synuclein accumulates in oligodendrocytes as GCIs in an age-dependent manner during MSA

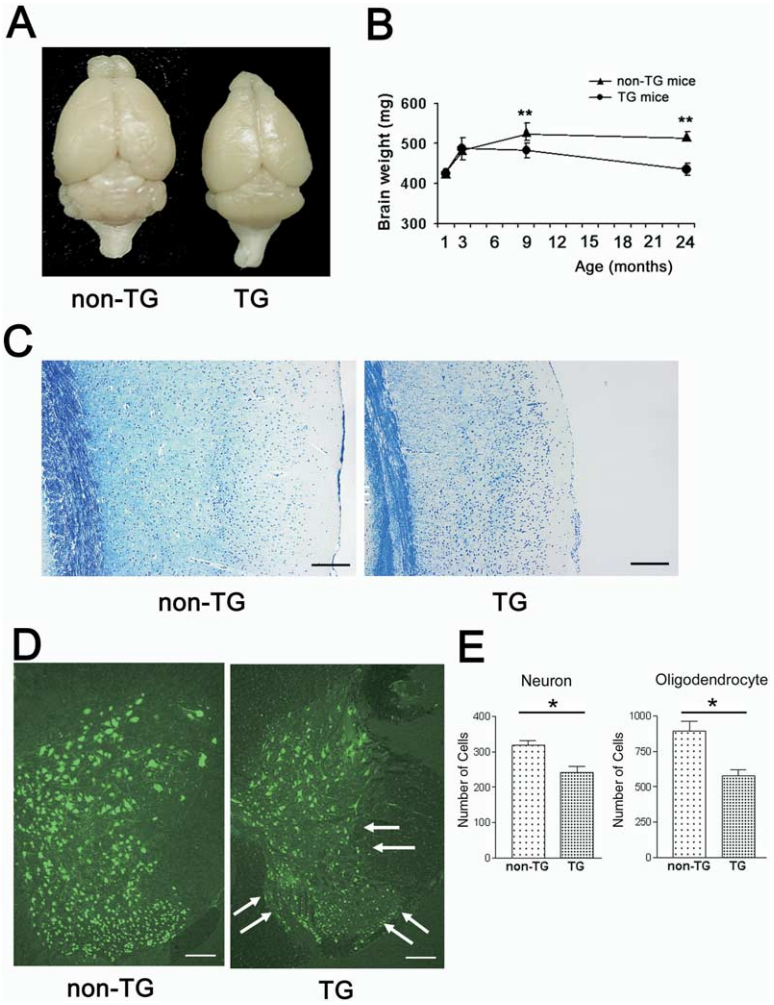

Figure 3. Expression of α-Synuclein in Oligodendrocytes Causes Brain Atrophy

(A) At 24 months of age, gross brain atrophy is evident in M2 Tg mice.

(B) Brain weight is progressively reduced in M2 mice. Error bars show the standard error of the means. **$p < 0.01$.

(C) Microscopic features of brain atrophy in 24-month-old M2 mouse compared to age-matched non-Tg control mice using Luxol fast blue stain with cresyl violet. In the atrophic brain of M2 mouse, note that the neuropil in the cerebral cortex is shrunk, and the white matter is reduced. Scale bar, 200 μm.

(D) Immunofluorescence study using NeuN shows a decrease of neurons in the spinal cord of 24-month-old M2 mice compared to age-matched non-Tg mice. Arrows show significant decreases of neurons, especially in the areas of lateral and medial columns of the spinal cord in the M2 mice. Scale bar, 150 μm.

(E) Bar graphs comparing the numbers of neurons and oligodendrocytes in the spinal cord of the M2 and non-Tg control mice. The number of the neurons and oligodendrocytes are reduced in the M2 mice. *$p = 0.024$ (neuron), *$p = 0.018$ (oligodendrocyte), Student's t test.

progression, we compared the α-synuclein inclusions in our M2 mice with GCIs from MSA patients, and we found that many of the α-synuclein aggregates in M2 mice resembled authentic GCIs in MSA (Figures 4A and 4B). Moreover, like MSA, α-synuclein accumulations also occurred in the neuropil (Figure 4A and Figure 1C). Although neuronal perikarya in the brain and spinal cord of M2 mice showed no immunoreactive α-synuclein aggregates, a Mab specific for highly phosphorylated high-apparent molecular weight (Mr) neurofilament subunit (NF-H) proteins (RMO24) showed strong phosphorylated NF-H immunoreactivity in neuronal perikarya in addition to axons (Figures 4C and 4D; Figures S2A and S2B). Since phosphorylated NF-H proteins normally are found only in axons and not in neuronal perikarya, but a redistribution of highly phosphorylated NF-H from axons to perikarya has been linked to neuronal injury (Sternberger et al., 1985; Goldstein et al., 1987), we conclude that NF-H-positive neurons in our M2 mice are injured and possibly degenerating. This view is also supported by the detection of axonal spheroids with RMO24 in the cortex of M2 mice indicative of axonal degeneration (Figure 4E), and these spheroids were not seen in control animals (Figure 4F). Other evidence in support of degeneration included remarkable gliosis in the brain as well as in the spinal cord detected by an anti-GFAP antibody using immunohistochemistry (Figures 4G and 4H; Figures S2C and S2D). In addition, aberrant growth-associated protein 43 (GAP43) immunoreactivity surrounding neuronal perikarya, which is distinctly abnormal and indicative of axons and dendrites undergoing regeneration after injury, was also detected by an antibody against GAP43 (Figure 4I). Significantly, similar abnormal neuronal perikaryal reactivity to anti-GAP43 antibody was observed in Purkinje cells of human MSA brains (Figure 4K). In spinal cord of age-matched control mice and Purkinje cells of human controls, anti-GAP43 antibody did not show immunoreactivity (Figures 4J and 4L).

Insoluble α-Synuclein Accumulates in an Age-Dependent Manner in M2 Mice

Since insoluble aggregated α-synuclein accumulates in brains of MSA patients, we serially extracted α-synuclein from brains of M2 mice using methods similar to those developed for the extraction of human MSA brain tissue (Duda et al., 2000a). Following the sequential extraction of CNS tissue with buffers of

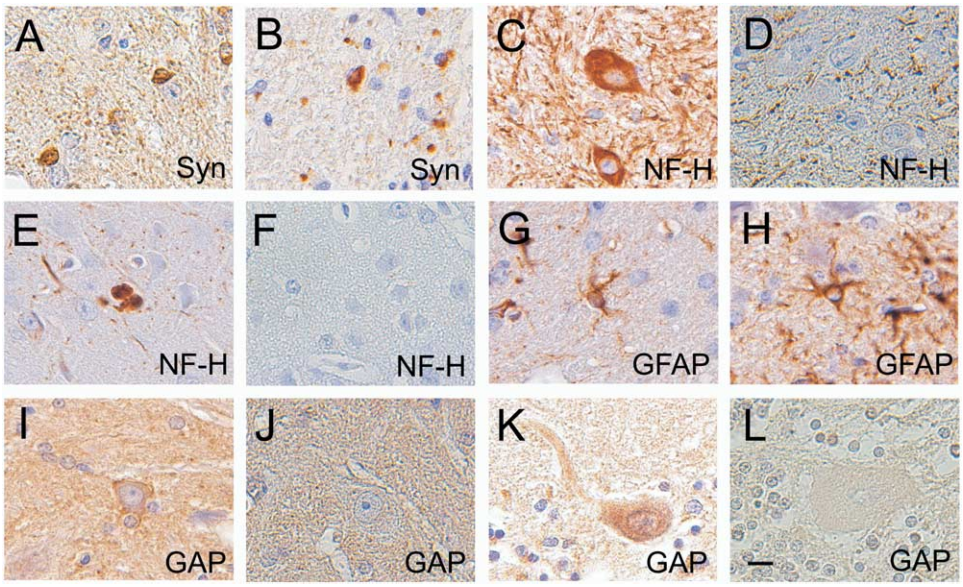

Figure 4. Pathological Changes in the CNS of M2 Tg Mice

(A and B) Immunohistochemical staining of tissue sections of cerebral white matter from 24-month-old M2 mice (A) and patients with MSA (B) using anti-α-synuclein antibody (Syn). Note the presence of GCI-like inclusions as well as the accumulation of α-synuclein in oligodendrocytes and the neuropil in M2 mice (A). These inclusions are similar to GCIs in patients with MSA (B).

(C and D) Numerous neurons of the spinal cord of M2 mice are immunoreactive for hyperphosphorylated neurofilament (NF-H) using RMO24 antibody (C), but neurons of age-matched control mice do not show any immunoreactivity with the RMO24 antibody (D).

(E and F) Axonal spheroids in the cerebral cortex of M2 mice are demonstrated by RMO24 staining (E), but no spheroids are found in the cerebral cortex of age-matched control mice (F).

(G and H) Anti-GFAP staining shows gliosis in the cerebral cortex (G) and spinal cord (H) of M2 mice.

(I and J) Neuronal perikarya in M2 mice are immunoreactive to anti-GAP43 antibody (GAP) (I), but no neuronal staining of anti-GAP43 antibody is shown in age-matched control mice (J).

(K and L) A Purkinje cell in the affected cerebellum of an MSA patient shows immunoreactivity to anti-GAP43 antibody (K), but no Purkinje cell in human controls shows similar immunoreactivity (L). Scale bar, 10 μm.

increasing protein extractability, human α-synuclein in CNS samples of M2 mice at the ages of 6, 12, 18, and 24 months were assayed by immunoblotting. Spinal cord and different brain regions (i.e., cerebrum, cerebellum, brain stem) were examined separately, and each region was serially extracted into three fractions of high salt (HS), RIPA, and formic acid (FA). Immunoblots of fractions from all four of these CNS regions of M2 mice were performed using the Mab Syn204, and this antibody detected human α-synuclein expression in all regions examined (Figures 5A and 5B). Since human α-synuclein was expressed at higher levels in the spinal cord and cerebrum, insoluble α-synuclein was also detected in FA fractions of these regions (Figures 5A and 5B). Some high-Mr insoluble α-synuclein species did not enter the resolving SDS-PAGE gels, and they began to accumulate in the CNS of M2 mice at 6 months of age and increased significantly in the spinal cord of 12-month-old and older mice (Figure 5B). Aggregated α-synuclein was partially resistant to FA solubilization, as shown by multiple bands of high-molecular mass species on the immunoblots (Figures 5A and 5B). Similar profile of α-synuclein insoluble aggregates were also detected by SNL1, a α-synuclein antibody that recognized both human and mouse α-synuclein in M2 but not in non-Tg mice (Figure 5B).

To compare the α-synuclein insolubility in M2 mice with that in MSA patients, samples of pons from patients with MSA and human controls were similarly extracted sequentially into three fractions of HS, RIPA, and FA. Immunoblotting with anti-α-synuclein Mab detected multiple bands of insoluble α-synuclein (including high-Mr aggregates at the top of gels) in the FA fraction of MSA but not in the pons of control patients (Figure 5C). Thus, the pattern of FA-extracted insoluble human α-synuclein from MSA brains and from our M2 mice bear striking similarities.

α-Synuclein-Induced Oligodendrocytic Degeneration Causes Demyelination and Secondary Axonal Degeneration

The effects of human α-synuclein accumulation and aggregation on oligodendrocytes were assessed ultrastructurally. Samples of cerebrum, pons, cerebellum, and spinal cord in M2 mice at the ages of 10 and 24 months were examined using transmission electron microscopy (EM) (Figure 6) and immuno-EM (Figure 7). Oligodendrocytes, which were immunoreactive with human-specific anti-α-synuclein Mab LB509 in preembedding immuno-EM (Figure 7G), contained degraded myelin and extensive accumulations of lysosomes (Figures 6A and 6B) as well as fragmented myelin in their cytoplasm (Figures 6C and 6D). This suggests that autophagocytosis of degenerated myelin occurred in dis-

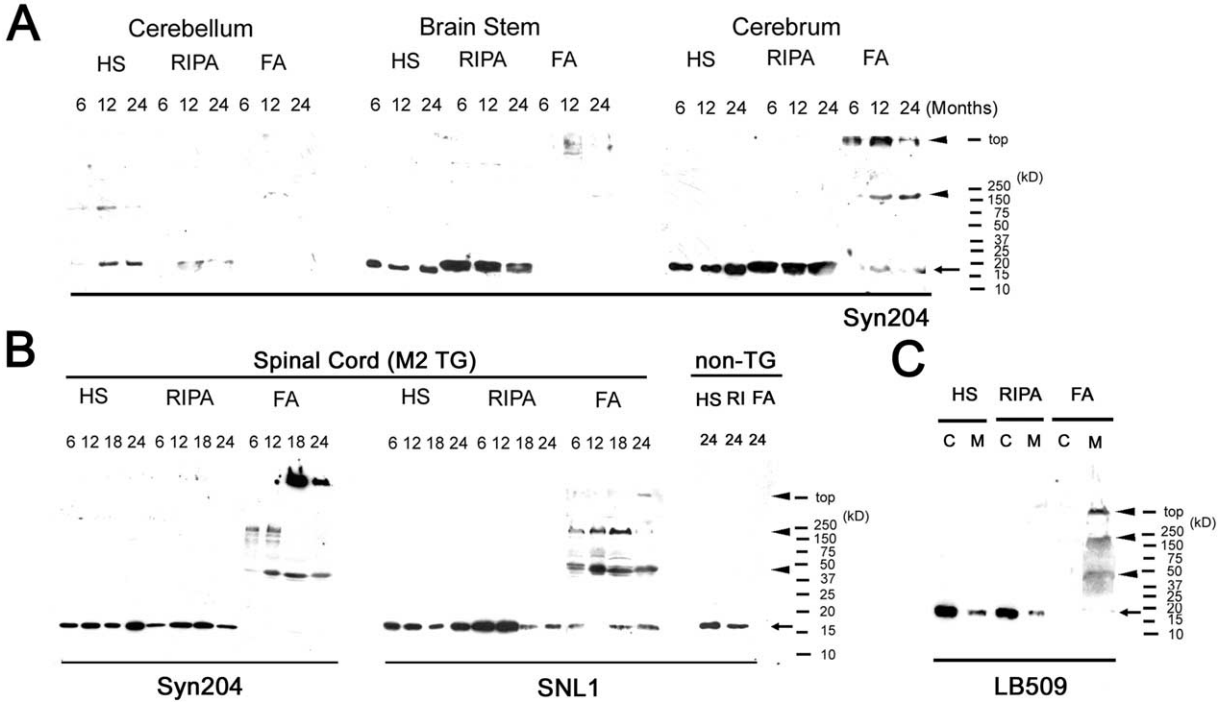

Figure 5. Insoluble α-Synuclein Accumulates in CNS of M2 Mice

(A) The CNS of M2 mice at the age of 6 months, 12 months, and 24 months was divided into four regions: cerebrum, cerebellum, brain stem, and spinal cord. Tissues from all four regions were sequentially extracted with HS, RIPA, and FA as described in the Experimental Procedures. Immunoblotting analysis with the human α-synuclein-specific antibody Syn204 shows insoluble α-synuclein in the FA fractions of the 12- and 24-month-old M2 mice (arrow) in addition to soluble α-synuclein in the HS and RIPA fractions. Aggregated α-synuclein that is resistant to FA appears as high-Mr bands within the resolving and stacking gels (arrowheads); since Syn204 is human α-synuclein specific, control mice showed no Syn204-immunoreactive bands (data not shown).

(B) Immunoblots of spinal cord serially extracted with HS, RIPA, and FA from M2 mice at the ages of 6, 12, 18, and 24 months and a non-Tg mouse at the age of 24 months conducted with Syn204 and SNL1. Insoluble α-synuclein in the FA fraction appears as multiple bands, which include aggregated α-synuclein at the top of gels in M2 mice at the age of 12 months and older on the immunoblots when stained with Syn204 (arrowhead). Mr is indicated on the right.

(C) Pontine tissues of MSA patients (M) and human controls (C) were sequentially extracted with HS, RIPA, and FA. Immunoblot analysis of these extracts with LB509 antibodies shows that insoluble α-synuclein is detected only in the FA fraction of brain extracts from MSA patient (arrow). As compared to the insoluble α-synuclein in M2 mice, a similar pattern of aggregated α-synuclein is recognized as high-Mr multiple bands in MSA brain tissues (arrowheads). No insoluble α-synuclein is detected in the FA fraction of human controls. Mr is indicated on the right.

eased oligodendrocytes. α-synuclein immunopositive filaments were detected in the cytoplasm of oligodendrocytes in M2 mice (Figures 7A–7C and 7G), indicating that oligodendrocytic degeneration may result from the aggregation of α-synuclein in M2 mice. These GCI-like fibrillar aggregates contained filaments that were approximately 10–15 nm in diameter (Figure 7C). Degenerated myelin sheaths associated with degenerating axons were observed in the CNS, most prominently in the spinal cord (Figure 6E). Accumulation of α-synuclein also was found within the degenerating myelin sheath (Figure 7H).

Neuronal cell bodies were not immunostained with any of anti-α-synuclein antibodies in M2 mice (Figure 7F and data not shown). Unexpectedly, SNL1, an antibody that recognizes endogenous mouse synuclein, detected α-synuclein ectopically deposited within a large number of axons (Figure 7E). Indeed, 73% of the total axons counted (n = 895) in the spinal cord of M2 mice at 24 months of age were immunostained by SNL1. However, in the spinal cord of age-matched controls, immuno-EM detected α-synuclein immunoreactivity with SNL1 only very rarely in axons (1.8% of the total axons; n = 538). Significantly, LB509, a Mab specific for human α-synuclein, did not immunostain axons of M2 mice or the brains and spinal cords of control mice. Thus, we conclude that endogenous mouse α-synuclein recognized by SNL1 ectopically accumulated within CNS axons of the M2 mice. To further characterize the nature of this accumulation, we conducted higher-power immuno-EM with SNL1 and showed that endogenous mouse α-synuclein accumulated as fibrils within axons in M2 mice (Figures 7J and 7K).

Ultrastructural analysis of spinal ventral roots in M2 and non-Tg control mice showed a loss of myelinated axons and sprouting of unmyelinated axons in M2 mice (Figures 6J–6L), indicating neuronal degeneration in the anterior horn of the spinal cord. Indeed, degenerative changes also were detected by EM in spinal cord neurons of M2 mice (Figure 7F). Taken together, these data

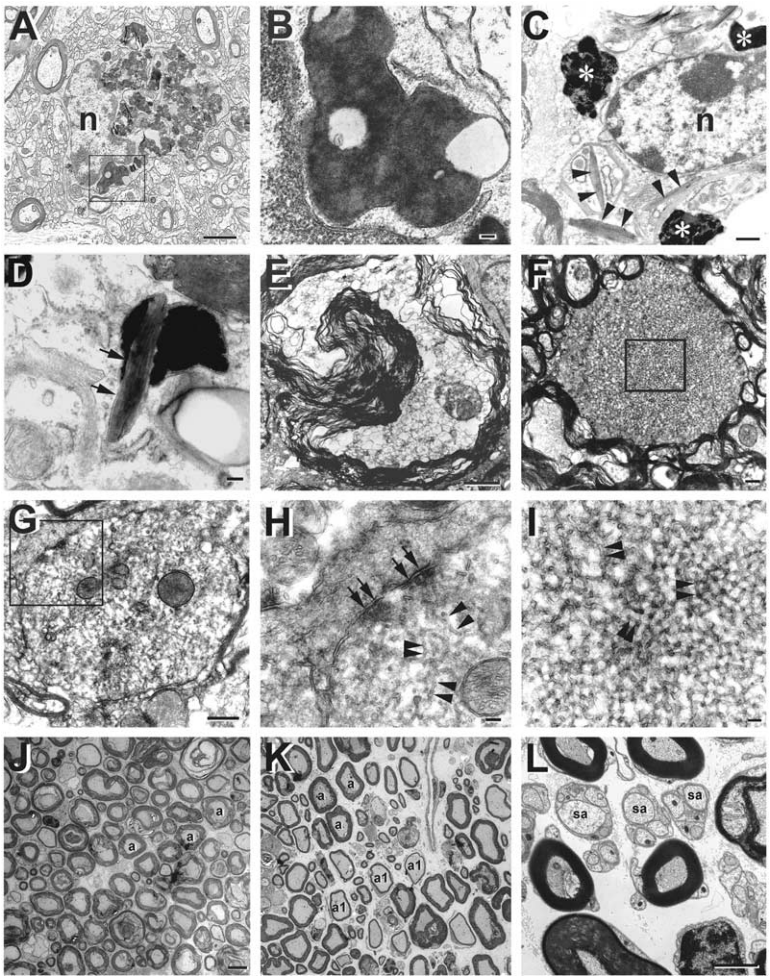

Figure 6. Transmission EM Analysis of M2 Mice

(A) A degenerating oligodendrocyte in cerebral cortex of a 24-month-old M2 mouse. The cytoplasm is largely occupied by secondary lysosomes. The nucleus (n) is irregular. (B) Higher magnification of a secondary lysosome in the oligodendrocyte shown in (A) also demonstrates that the lysosomes contain lamellar structures of degenerated myelin. (C) An oligodendrocyte in the spinal cord of a 24-month-old M2 mouse displaying unusual pathological organelles, including fragmented myelin and some rod-like cytoplasmic structures (arrowheads). There also are secondary lysosomes in the cytoplasm (asterisks). (D) High-power magnification of an oligodendrocyte, revealing a lysosome associated with fragmented myelin in the cytoplasm (arrows), indicating autophagocytosis of degraded myelin. (E) Micrograph showing degeneration of a myelinated nerve fiber in the spinal cord of a M2 Tg mouse. Note the dilated myelin sheath and the frayed layers of myelin in the enlarged space between the outer myelin and the axon. Also note that the remains of the axon within the degenerated myelin contain amorphous structures with enlarged mitochondria. (F) Low-power EM view of an abnormal inclusion in the spinal cord of an M2 mouse. The boxed area is seen at higher power in (I). The inclusion is surrounded by a membrane and is mostly occupied by disordered tubular structures. (G) Features of the inclusions are also observed in axon terminals of the spinal cord of M2 mice. The axon terminal contains synaptic junctions and degenerated synaptic vesicles, abnormally large vesicles and mitochondria. The terminal is mostly occupied by disordered tubules. (H) A higher-power view of the boxed-in area in (G), which confirms synaptic junctions in the axon terminal (arrows). The disordered tubules in the terminal are approximately 20–35 nm in diameter (arrowheads), and they are also immunolabeled with the anti-α-synuclein antibodies (see Figure 7O). (I) High-power view of boxed-in area in (F), showing that the inclusion is comprised of disordered tubules (arrowheads) and amorphous dense structures among the tubules. The tubules are approximately 20–35 nm in diameter, and each shows a dense wall surrounding a lighter core when they are sectioned transversely. (See Figure 7O for immunolabeled tubules). (J–L) Transverse sectioned ventral roots of 24-month-old M2 (K and L) and age-matched non-Tg (J) mice. In M2 mice (K), the density of myelinated axons (a) is decreased, and some of the myelinated axons have thin myelin (a1). Magnifications of (J) and (K) are the same. In high magnification of the ventral root of M2 mice, sprouting axons (sa) are seen by bundles of small, closely packed unmyelinated axons, indicative of axonal degeneration (K). Scale bars, 10 μm (J); 2 μm (A, E, and L); 500 nm (C, F, and G); and 100 nm (B, D, H, and I).

show that axons accumulate endogenous mouse α-synuclein in response to human α-synuclein-induced oligodendrocytic degeneration in M2 mice.

Surprisingly, a different type of inclusion containing disordered tubular structures, approximately 25–35 nm in diameter, was identified in the spinal cord of M2 mice using transmission EM (Figures 6F and 6I). Since the same appearance of disordered tubular structures was observed in the degenerating axon terminals in the spinal cord (Figures 6G and 6H), these pathological inclusions may be derived from degenerating axon terminals. The degenerating axon terminals, which showed accumulations of α-synuclein (Figures 7I and 7L), increased in number and size in older M2 mice, and they were not observed in the brains (data not shown) and spinal cords of the age-matched non-Tg mice (Figure 7D). The axon-terminal inclusions were morphologically and immunochemically distinct from the oligodendrocytic inclusions (compare Figures 7A–7C with Figures 7M–7O). For example, while the human α-synuclein fibers in the oligodendrocytic inclusions were stained with the human-specific anti-α-synuclein Mab LB509 (Figures 7B and 7C), the tubular structures in the axon-terminal inclusions were not decorated by LB509 but instead only reacted with the antibodies that recognized both endogenous mouse and human α-synucleins (SNL1) (Figure 7O).

That mouse α-synuclein accumulated in axons and nerve terminals of M2 mice was further confirmed by immunohistochemistry in spinal cord sections using 7544, a mouse-specific α-synuclein antibody (Figures 8A and 8B). Since endogenous mouse α-synuclein is present at low level in the spinal cord, 7544 weakly immunostained spinal cord sections from non-Tg mice.

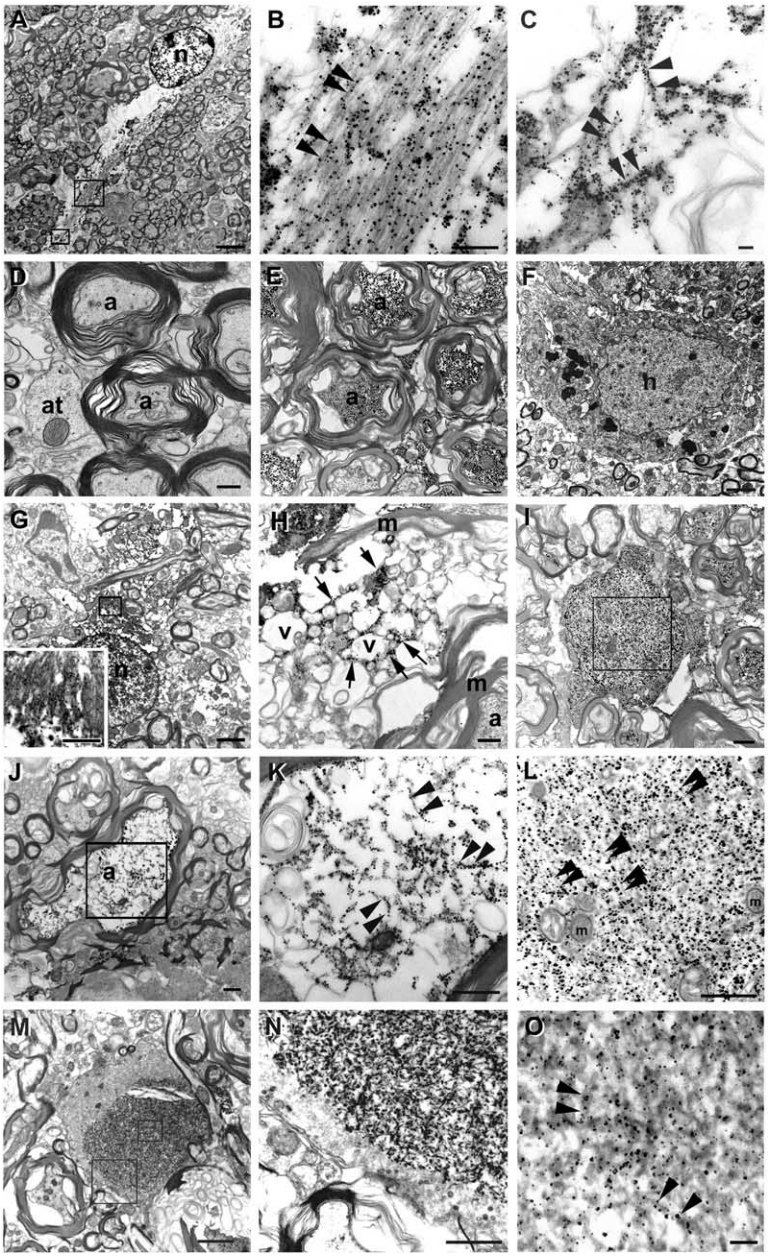

Figure 7. Immuno-EM Analysis of M2 Mice

(A) Accumulation of α-synuclein in an oligodendrocyte in the spinal cord of a 24-month-old M2 mouse. Anti-α-synuclein antibody, Syn204, detects fibrillary accumulation of α-synuclein in the cytoplasm and the process. (B) Higher magnification of the inclusion in the large boxed-in area in the oligodendrocyte in (A), showing fibrillary inclusions (arrowheads). (C) Higher magnification of the process of the oligodendrocyte in the small boxed area in (A). Fibrils of α-synuclein are approximately 10–15 nm in diameter and are morphologically distinguished from the disordered tubules that make up the inclusions found in axon terminals (see Figure 7O). (D and E) Immunoreactivity of SNL1, an anti-α-synuclein antibody that recognizes mouse endogenous α-synuclein, in axons (a) of spinal cord of 24-month-old M2 (E) and age-matched non-Tg control (D) mice. Immunodetection with SNL1 reveals that α-synuclein ectopically accumulates within axons of M2 TG mice (E). SNL1 displays no immunoreactivity in axons (a) or axon terminal (at) in control non-Tg mice (D). (F) α-synuclein is not detected in neuronal perikarya in the spinal cord of an M2 mouse. A neuron is darkened, and the cytoplasm contains vacuoles, indicating neuronal degeneration. (G) α-synuclein accumulation in an oligodendrocyte in the spinal cord of a 24-month-old M2 mouse detected by LB509, a human-specific anti-α-synuclein antibody. Human α-synuclein is detected in the cytoplasm and its inclusion of the oligodendrocyte but is not detected in the axons. Higher magnification of the inclusion in the boxed area is shown in the inset in the left lower corner (scale bar, 500 nm). The inclusion contains α-synuclein fibrils. (H) SNL1 shows α-synuclein accumulation within degenerating myelin of an M2 mouse spinal cord. α-synuclein has accumulated in degenerating myelin (m) with vacuoles (v) (arrows). The axons (a) show ectopic accumulation of α-synuclein. (I) A degenerating axon terminal in the spinal cord of a 24-month-old M2 mouse demonstrates strong immunoreactivity to SNL1. (J) Ectopic accumulation of α-synuclein in an axon (a) forms fibrils in the spinal cord of an M2 mouse detected with SNL1. (K) Higher magnification of the boxed area in the axon in (J) demonstrates that SNL1 detects individual fibrils, approximately 10–15 nm in diameter (arrowheads). (L) Higher magnification view of the degenerating axon terminal in the boxed area in (I) shows that the terminal is enlarged by accumulation of α-synuclein fibrils (arrowheads) and disordered tubular structures with mitochondria (m). (M) An abnormal inclusion in axon terminal in the spinal cord of a 24-month-old M2 mouse is stained with SNL1. (N) Middle magnification of the inclusion (M) shows that the inclusion is mostly composed by disordered tubules. (O) In high magnification of the inclusion (M), the inclusion contains 25–35 nm tubules that are immunolabeled with SNL1 (arrowheads). Scale bars, 2 μm (A, F, G, and M); 500 nm (B, D, E, H–L, and N); and 100 nm (C and O).

In sharp contrast, 7544 detected mouse α-synuclein in axons and in axonal terminals around spinal cord motor neurons in M2 Tg mice. These accumulations of mouse α-synuclein in the spinal cord of M2 mice are specific, since anti-synaptophysin antibodies did not immunostain these aberrant nerve terminals but weakly stained the degenerating axons (data not shown). Furthermore, increased mouse α-synuclein at synaptic terminals in the hippocampus of M2 mice was detected by SNL1 when compared with non-Tg mice (Figures 8C and 8D). Taken together, these data suggest that the α-synuclein inclusions that we observed here in the degenerating axon terminals as well as within the axons of M2 mice were comprised of endogenous mouse α-synuclein.

Discussion

We have demonstrated here that the M2 Tg mice expressing human α-synuclein in oligodendrocytes exhibited a primary oligodendrocytic as well as a secondary neuronal degenerative phenotype with motor impairments similar to MSA. This motor behavioral defi-

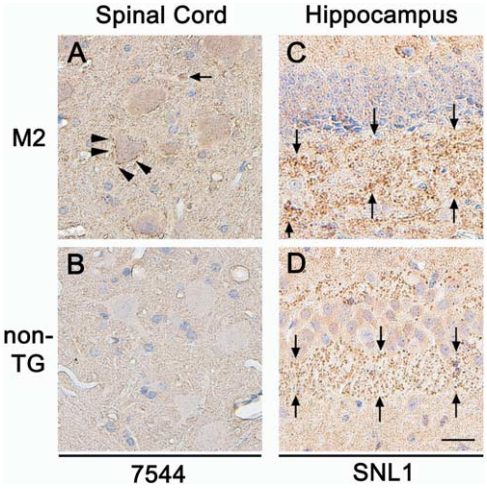

Figure 8. Abnormal Accumulation of Endogenous Mouse α-Synuclein in Axons and Axon Terminals of M2 Mice

(A and B) Immunohistochemical study using 7544, a mouse α-synuclein-specific antibody in the spinal cord of 24-month-old M2 (A) and age-matched non-Tg mice (B). Note that α-synuclein immunoreactivity was detected in the nerve terminals (arrowheads) and axonal inclusions (arrow) but not in the oligodendrocytes of the M2 mouse.

(C and D) SNL1 detected more α-synuclein immunoreactivities in synaptic terminals of M2 hippocampus (C) than in those of non-Tg control (D). Scale bar, 6 μm.

cit was associated with the accumulation of human α-synuclein aggregates in oligodendrocytes as well as endogenous mouse α-synuclein in axons and axon terminals. M2 mice showed progressive brain atrophy, and immunohistochemistry using anti-α-synuclein antibodies demonstrated that M2 mice developed GCI neuropathology similar to MSA. Biochemical analyses of sequentially extracted CNS tissues of M2 mice using buffers of increasing strengths showed accumulations of insoluble α-synuclein. Similar high-Mr species of insoluble α-synuclein (Tu et al., 1998; Dickson et al., 1999; Duda et al., 2000a), including the presence of α-synuclein aggregates at the top of gels, have been detected in brains of MSA patients and in our M2 mice using immunoblots. Although a Tg mouse expressing α-synuclein in oligodendrocytes driven by the proteolipid protein promoter (PLP) was shown to develop α-synuclein containing GCI-like inclusions, the formation of α-synuclein filaments, motor impairment, and secondary neurodegeneration was not reported in these Tg mice (Kahle et al., 2002). The lack of neurodegeneration in the PLP-α-synuclein Tg mice could be due to the different promoters used to drive α-synuclein expression or insufficient expression levels of α-synuclein in oligodendrocytes. Thus, our M2 mice not only recapitulated many features of MSA neuropathology but also provided evidence that secondary neuronal degeneration can occur as a direct consequence of oligodendrocytic GCI-like pathologies. This finding is extremely important in assessing the contribution of GCIs versus neuronal α-synuclein inclusions to the neurodegeneration in MSA, and our M2 mice would therefore serve as a useful Tg mouse model of MSA. Other examples of axonal degeneration mediated by glial pathologies include multiple sclerosis, which causes axonal degeneration with demyelination in human CNS (Trapp et al., 1998), and a hereditary form of peripheral neuropathy, which shows axonal involvement with myelin degeneration (Bergoffen et al., 1993), while axonal degeneration also was demonstrated in PLP-deficient mice (Griffiths et al., 1998).

We observed significant oligodendroglia and neuron loss in spinal cord and cortical areas in the M2 mice, and the distribution of neuronal loss in the spinal cord showed similarity to human MSA pathology (Papp and Lantos, 1994). The lack of overt degeneration in cerebellum and the pontine nuclei may be due to the lower levels of α-synuclein expression, since our biochemical analyses showed much lower levels of α-synuclein in cerebellum than in cortex and spinal cord. We also observed significant demyelination in the M2 mice. Although pronounced demyelination in MSA was not observed using conventional methods such as Luxol fast blue, widespread myelin degeneration in MSA was observed using antibodies that recognized a specific epitope in human myelin basic protein (Matsuo et al., 1998). Thus, demyelination in M2 mice is another feature consistent with MSA.

Evidence was provided to document neuronal degeneration in our M2 Tg mice. For example, pathological changes were also observed in neuronal cell bodies, which accumulated phosphorylated NF-H immunoreactivity, a marker of neuronal injury, since the phosphorylated NF-H proteins are normally restricted to axons in healthy neurons. However, in several neurological diseases and in experimental models of axotomy, phosphorylated NF-H proteins have been detected in neuronal perikarya (Klosen et al., 1990), and therefore the translocation of phosphorylated NF-H from axons to cell bodies is a signature of the reaction of neurons to axonal injury (Hedreen and Koliatsos, 1994). Further evidence in support of axonal damage and hence axonal degeneration include the presence of phosphorylated NF-H-immunoreactive axonal spheroids and the increased expression of GAP43 in neurons of the M2 mice. Significantly, similar neuronal changes also were observed in the brains of MSA patients here. Ultrastructural studies of the spinal cord and ventral root demonstrated axonal sprouting indicating axonal and neuronal degeneration in M2 mice.

Transmission EM and immuno-EM analyses using anti-α-synuclein antibodies demonstrated that two types of inclusions coexisted in the CNS of M2 mice. One type of α-synuclein aggregate was found in the cytoplasm of oligodendrocytes associated with degeneration. These inclusions were filamentous, as demonstrated by immuno-EM, and they resulted from the accumulation of human α-synuclein that was expressed in the oligodendrocytes under the control of the CNP promoter. Ultrastructurally, these filamentous inclusions resembled those identified in Tg mice expressing human A53T α-synuclein in neurons under control of the PrP promoter (Giasson et al., 2002). A second type of inclusion localized to the axons and axon terminals had a tubular ultrastructural appearance, in which endogenous mouse α-synuclein was a component. Accumulation of the endogenous

mouse α-synuclein also was detected in the degenerated axon terminals and the axons themselves, indicating axonal degeneration. However, it is unclear why endogenous mouse α-synuclein accumulated selectively within axons and their terminals. It is possible that this may represent a specific neurodegenerative response to human α-synuclein-induced oligodendroglia degeneration, or a regenerative response to axonal injury caused by degenerating oligodendrocytes. Nevertheless, since the most distal segment of the axon affected was the axon terminal, which is where α-synuclein is physiologically localized (George et al., 1995; Iwai et al., 1995; Jakes et al., 1994), aggregation of neuronal mouse α-synuclein likely begins at axon terminals. Morphologically, the axon-terminal inclusions occupied by the disordered tubules show some resemblance to the microtubular accumulations reported in GCIs of MSA patients (Nakazato et al., 1990; Yamada and McGeer, 1990).

M2 mice exhibited another interesting feature of the MSA phenotype, since they also showed motor impairments between 7 and 9 months of age and developed pathology in the CNS between 3 and 10 months of age. Thus, the onset of degeneration is suspected to be between 3 and 6 months of age in the M2 mice. Although M2 mice showed an early onset of the disease process, these mice did not show any statistically significant difference in life span compared to non-Tg mice. For this reason, we speculate that the motor impairments in M2 mice were sufficiently mild such that they did not compromise the life span of these mice and/or that the disease process in the M2 mice is slow. Because the disease is progressive in the CNS and the onset is very early in the life span of the M2 mice, the latter explanation seems more plausible. It is clear that the M2 mice survive longer than Tg mice overexpressing human A53T α-synuclein under the control of the PrP promoter, since 100% of the latter mice die between 7 and 16 months (Giasson et al., 2002).

The slow disease progression seen in M2 mice may be explained as a two-step process; oligodendrocytic degeneration occurs first, and axonal degeneration occurs second. Since axonal degeneration is an indirect process related to the oligodendrocyte pathology, axonal neuropathology may take longer to develop. The slowly progressive disease course also was characterized by autophagocytosis in the oligodendrocytes and unique structural inclusions in the axon terminals. Although oligodendrocytes are known to form myelin sheaths by their processes (Peters et al., 1991), autophagocytosis of fragmented myelin is a pathological feature that is rarely observed under normal conditions. The M2 mouse line may be a very informative animal model for studying and understanding human neurodegenerative disease mechanisms, since human neurodegeneration commonly progresses slowly as well.

In conclusion, although the initiating mechanisms of neurodegeneration in MSA remain to be elucidated, the data from the analyses of the M2 mice support the notion that oligodendrocytic degeneration as a consequence of α-synuclein inclusion formation contributes to secondary neuronal degeneration observed in this mouse model, thereby suggesting that GCIs play a similar role in MSA. Thus, the M2 mice are compelling models for elucidating mechanisms of disease in MSA and of glial-mediated neuronal degenerative processes in humans.

Experimental Procedures

Generation of Tg Mice

The generation of Tg mice that express human α-synuclein in CNS oligodendrocytes driven by the murine CNP promoter was described previously (Giasson et al., 2003). Three stable Tg lines carrying human α-synuclein were established, and Tg offspring were identified by Southern blot analysis using mouse tail DNA. However, only the M2 line expressed sufficient human α-synuclein to be significantly detected by immunoblots using human-specific anti-α-synuclein antibodies from brain homogenates, and a homozygous Tg lineage was identified by quantitative Southern blot analysis and verified by backcrossing to non-Tg mice.

Isolation of RNA and Northern Blotting

Total brain RNA from non-Tg and M2 Tg mice or the mouse prion protein promoter (line M7) (Giasson et al., 2002) was isolated using TRIzol reagent (Invitrogen Life Technologies, Carlsbad, CA). The amounts of RNA were determine by optical density at λ = 260 nm. RNA (10 or 100 μg) was electrophoresed on 1% formaldehyde agarose gel and blotted onto Hybond-N nitrocellulose membrane (Amersham Biosciences, Piscataway, NJ). Prehybridization and hybridization were performed in Church buffer (0.5 M sodium phosphate [pH 7.2], 1 mM EDTA, 7% SDS) and 0.5 mg/ml salmon sperm DNA at 65°C. The membranes were incubated with an equal amount of ^{32}P-labeled probes generated by random oligonucleotide priming and extension of isolated full-length mouse and human α-synuclein cDNAs. The membranes were washed with 0.1% SDS/0.1× SSC (15 mM NaCl, 1.5 mM Na citrate [pH 7.0]) at 65°C, air dried, and exposed to a PhosphorImager plate (Amersham Biosciences, Piscataway, NJ).

In Situ Hybridization

Three specific oligonucleotide probes were designed for human and mouse α-synuclein. The two 40 base probes used to specifically detect the Tg transcript of human α-synuclein are TGGCT GGCAACTAGAAGGCACAGTCGAGGCTGATCAGCGG, complementary to the BGH sequence, and CCCCTCGAGGTCGACGGTATCG ATAAGCTTGGATGGAACA, complementary to the pcDNA3.1 plasmid sequence. The 40 base probe specific for mouse α-synuclein used is GGGGAGCACCGGGATGCTGAGGGGCAGGTACAGGACG CCG, complementary to bases 141 to 180 from the terminal of exon 6 of the mouse α-synuclein sequence (GenBank accession number AF179272).

Labeling of probes with [α-^{33}P]dATP and in situ hybridization was performed exactly as previously described (Vogelsberg-Ragaglia et al., 2001).

Motor Testing

Rotarod Treadmill Test

The accelerating rotarod treadmill (Ugo Basile, Italy) was used to analyze motor function of M2 mice. Mice were given three trials with 45 min intertrial intervals on each of 2 consecutive days for 3 weeks. Each animal's endurance time (AET) was recorded, and the average of AETs is calculated in Figure 2. Sixty-six M2 mice were used for the rotarod test (30 male and 34 female), and 62 non-Tg mice were used for comparison (28 male and 34 female). In addition, 6-week-old M2 (n = 14) and non-Tg control mice (n = 10) were habituated on the rotarod and then were tested consecutively every week from 7 weeks of age until 32 weeks of age.

Wire Hanging Grip Strength Test

Mice were placed with their forepaws on a horizontal wire and were allowed to grasp the wire and remain suspended. Each mouse was given two trials with an intertrial interval of 2 hr. The total time the mice remained hanging on the wire was recorded as hanging times in seconds. Fifty-one M2 mice were used for this grip strength test (24 male and 27 female), and 45 non-Tg mice were used for comparison (22 male and 23 female).

Anti-α-Synuclein Antibodies

Syn204 is a Mab raised against recombinant human α-synuclein that selectively recognizes a human α-synuclein epitope between amino acid residues 87 and 110 (Giasson et al., 2000). SNL1 is a rabbit polyclonal antibody raised against a synthetic peptide corresponding to amino acids 104–119 in α-synuclein. SNL1 detects both mouse and human α-synuclein (Giasson et al., 2000). LB509 is a Mab that recognizes an epitope that includes amino acid residues 115–122 in human α-synuclein. LB509 does not react with mouse α-synuclein because of amino acid differences with human α-synuclein (Baba et al., 1998; Jakes et al., 1999). 7544, which specifically recognizes mouse α-synuclein, is a gift from Dr. P.J. Kahle (Adolf Butenandt Institute, Germany) (Kahle et al., 2000).

Analysis of Total α-Synuclein Protein and Immunoblot Analyses

Brains and spinal cords were dissected after mice were lethally anesthetized. For total protein extracts, CNS tissues were weighed and homogenized in 2% SDS buffer (2% SDS and 50 mM Tris-HCl [pH 7.5]) with protease inhibitor cocktail (1 mM PMSF and 1 μg/ml each of pepstatin-A, leupeptin, TPCK, TLCK, and soybean trypsin inhibitor). Protein concentration was determined using bicinchoninic acid assay (BCA) (Pierce, Rockford, Il). After the addition of SDS sample buffer, equal amounts of each sample were resolved on 13% SDS polyacrylamide gels, transferred onto nitrocellulose membranes, and processed for immunoblot analyses as previous described (Higuchi et al., 2002).

Serial Extraction of α-Synuclein in Mouse and MSA CNS

Mouse CNS was dissected into cerebrum, cerebellum, brain stem, and spinal cord. Each part of the CNS tissue was weighed and homogenized in 2 ml/g of high-salt (HS) buffer (50 mM Tris-HCl [pH 7.5], 10 mM EGTA, 5 mM $MgSO_4$, 750 mM NaCl, and 20 mM NaF) with protease inhibitor cocktail and centrifuged at 100,000 × g for 30 min at 4°C, where the supernatant was used as the HS-soluble fraction. The pellet was homogenized in 1 M sucrose in Tris-HCl (pH 7.6) and centrifuged at 100,000 × g for 30 min at 4°C to remove myelin and any related lipids. The resulting pellet was dissolved in RIPA (50 mM Tris-HCl [pH 8.0], 150 mM NaCl, 5 mM EDTA, 1% NP-40, 0.5% sodium deoxycholate, and 0.1% SDS) with protease inhibitors at 2 ml per gram wet weight of brain tissue and centrifuged at 100,000 × g for 30 min at 4°C. The RIPA-soluble supernatant was used as RIPA fraction. The pellet was then reextracted in 70% formic acid (FA) by sonication. Protein concentrations of HS and RIPA samples were determined using the BCA assay. FA samples were dried and resuspended in SDS sample buffer with volumes equivalent to 1 ml per gram wet weight of tissue. Immunoblot analyses were conducted as described above.

Brain tissues of MSA and control patients were sequentially extracted into HS, RIPA, and FA fractions to examine insoluble α-synuclein as described above for mouse CNS.

Immunohistochemical and Immunofluorescence Analyses of M2 Mice and Patients with MSA

Mice were perfused transcardially with phosphate-buffered saline (PBS) after being lethally anesthetized. Brains and spinal cords were fixed in 10% neutral buffered formalin or 70% ethanol/150 mM NaCl. Following paraffin infiltration, 6 μm thick sections were prepared. Sections were blocked with 2% fetal bovine serum in 0.1 M Tris (pH 7.5) and incubated overnight at 4°C with primary antibodies: anti-α-synuclein antibodies (Syn204, SNL1, LB509, 7544), a Mab specific for hyperphosphorylated NF-H (RMO24) (Schmidt et al., 1991), anti-GFAP antibody (DAKO, Denmark), or anti-GAP43 antibody (Sigma, St. Louis, MO). Sections were reacted with biotinylated-conjugated secondary antibodies and developed with diaminobenzidine (DAB) using Vectastain ABC kit (Vector Laboratories, Burlingame, CA) as previously described (Trojanowski et al., 1989). Brain tissues of five autopsy-confirmed MSA patients (Tu et al., 1998; Gilman et al., 1999) and five age-matched controls also were examined by immunohistochemistry.

Double-labeling immunofluorescence study was conducted to demonstrate the colocalization of the human α-synuclein transgene and endogenous CNP in oligodendrocytes. To do this, M2 and non-Tg mice were serially perfused with 10 ml of PBS, 25 ml of 3% paraformaldehyde in 0.1 M phosphate buffer (PB; pH 7.5), 25 ml of 3% paraformaldehyde in 50 mM sodium borate buffer (pH 9.0), and 30 ml of 10% sucrose in 0.1 M PB as described elsewhere (Higuchi et al., 2002). The 15 μm thick sections of frozen brain and spinal cord were double immunostained with anti-α-synuclein (SNL1) and anti-CNP antibodies.

Quantitative Analysis of Neurons and Oligodendrocytes

The total number of neurons in the L2 lumbar spinal cord as well as dopaminergic neurons in the substantia nigra was counted on sections from 24-month-old M2 and age-matched non-TG mice (each for n = 3, 8 sections from each mouse). Cells were visualized by immunostaining with NeuN (Chemicon, Temecula, CA), an antibody that labels neuronal nuclei, and tyrosine hydroxylase (TH) (Pel-Freese, Brown Deer, WI). Quantitative analyses were conducted on the photographs that cover entire area of interest with an image analysis software, ImagePro^{Plus} (Media Cybernetics, Silver Spring, MD). For oligodendrocyte analysis, cells were visualized by immunostaining with anti-CNP antibody. The total number of cells in the lumbar spinal cord sections from the M2 and non-TG mice (each for n = 3, 8 sections) was manually counted.

Transmission EM

M2 and control mice at 10 and 24 months of age (n = 3 of each) were analyzed by transmission EM. The mice were deeply anesthetized and sacrificed by cardiac perfusion using 0.1 M cacodylate buffer (pH 7.4), followed by 4% paraformaldehyde and 2% glutaraldehyde. Cerebrum, pons, cerebellum, and lower thoracic spinal cord were fixed for 18 hr. Tissues were postfixed with 2% osmium tetraoxide for 1 hr and dehydrated and embedded in Epon. Ultrathin sections were cut and observed with a Joel 1010 transmission electron microscope (Peabody, MA).

Preembedding Immuno-EM

M2 and control mice at 10 and 24 months of age (n = 3 of each) were anesthetized and perfused with 0.1 M cocadylate buffer (pH 7.5), followed by 2% paraformaldehyde and 0.5% glutaraldehyde. Cerebrum, pons, cerebellum, and spinal cord tissues were fixed for 6 hr, washed in PBS, and cut into 50 μm thick sections with a vibratome. The sections were incubated in 0.1% sodium borohydride in PBS for 15 min and blocked with a solution of 5% fetal bovine serum, 1% bovine serum albumin, and 0.2% cold water fish skin gelatin in PBS for 2 hr. The sections then were incubated overnight at 4°C with primary antibodies: anti-α-synuclein antibodies (Syn204, LB509, or SNL1) or anti-synaptophysin antibody (Covance, Richmond, CA). The sections were incubated with biotinylated-conjugated secondary antibodies and developed with diaminobenzidine using Vectastain ABC kit as described above. The sections were silver enhanced as described by Rodriguez et al. (1984). The sections were dehydrated and embedded in epoxy resin. Ultrathin sections were cut and observed using a Joel 1010 electron microscope.

Supplemental Data

The Supplemental Data include two supplemental figures and can be found with this article online at http://www.neuron.org/cgi/content/full/45/6/847/DC1/.

Acknowledgments

Supported by grants from the National Institutes of Health (AG-09215, NS-044233). V.M.-Y.L. is the John H. Ware III Chair in Alzheimer's Disease Research, and B.I.G. was the recipient of a fellowship from the Canadian Institutes of Health Research. I.Y. is the recipient of a grant from Okinaka Memorial Institute for Medical Research and the Naito Foundation. J.Q.T. is the William Maul Measey-Truman G. Schnabel, Jr. Chair of Geriatric Medicine and Gerontology. We would like to thank the Biomedical Imaging Core Facility of the University of Pennsylvania for assistance in the EM studies, E.H. Norris for reading the manuscript, Lauren Zeitels for technical assistance, Dr. M. Gravel (McGill University, Montreal,

Canada) for kindly providing the CNP promoter vector, and the families of patients who make this research possible.

Received: June 10, 2004
Revised: November 29, 2004
Accepted: January 21, 2005
Published: March 23, 2005

References

Arima, K., Ueda, K., Sunohara, N., Arakawa, K., Hirai, S., Nakamura, M., Tonozuka-Uehara, H., and Kawai, M. (1998). NACP/α-synuclein immunoreactivity in fibrillary components of neuronal and oligodendroglial cytoplasmic inclusions in the pontine nuclei in multiple system atrophy. Acta Neuropathol. (Berl.) *96*, 439–444.

Baba, M., Nakajo, S., Tu, P.H., Tomita, T., Nakaya, K., Lee, V.M.-Y., Trojanowski, J.Q., and Iwatsubo, T. (1998). Aggregation of α-synuclein in Lewy bodies of sporadic Parkinson's disease and dementia with Lewy bodies. Am. J. Pathol. *152*, 879–884.

Bergoffen, J., Scherer, S.S., Wang, S., Oronzi Scott, M., Bone, L.J., Paul, D.L., Chen, K., Lensch, M.W., Chance, P.F., and Fischbeck, K.H. (1993). Connexin mutations in X-linked Charcot-Marie-Tooth disease. Science *262*, 2039–2042.

Clement, A.M., Nguyen, M.D., Roberts, E.A., Garcia, M.L., Boillee, S., Rule, M., McMahon, A.P., Doucette, W., Siwek, D., Ferrante, R.J., et al. (2003). Wild-type nonneuronal cells extended survival of SOD1 mutant motor neurons in ALS mice. Science *302*, 113–117.

Dickson, D.W., Liu, W.-K., Hardy, J., Farrer, M., Mehta, N., Uitti, R., Mark, M., Zimmerman, T., Golbe, L., Sage, J., et al. (1999). Widespread alteration of α-synuclein in multiple system atrophy. Am. J. Pathol. *155*, 1241–1251.

Duda, J.E., Giasson, B.I., Gur, T.L., Montine, T.J., Robertson, D., Biaggioni, I., Hurtig, H.I., Stern, M.B., Gollomp, S.M., Grossman, M., et al. (2000a). Immunohistochemical and biochemical studies demonstrate a distinct profile of α-synuclein permutations in multiple system atrophy. J. Neuropathol. Exp. Neurol. *59*, 830–841.

Duda, J.E., Lee, V.M.-Y., and Trojanowski, J.Q. (2000b). Neuropathology of synuclein aggregates: New insights into mechanisms of neurodegenerative diseases. J. Neurosci. Res. *61*, 121–127.

George, J.M., Jin, H., Woods, W.S., and Clayton, D.F. (1995). Characterization of a novel protein regulated during the critical period for song learning in the zebra finch. Neuron *15*, 361–372.

Giasson, B.I., Jakes, R., Goedert, M., Duda, J.E., Leight, S., Trojanowski, J.Q., and Lee, V.M.-Y. (2000). A panel of epitope-specific antibodies detects protein domains distributed throughout human α-synuclein in Lewy bodies of Parkinson's disease. J. Neurosci. Res. *59*, 528–533.

Giasson, B.I., Duda, J.E., Quinn, S.M., Zhang, B., Trojanowski, J.Q., and Lee, V.M.-Y. (2002). Neuronal α-synucleinopathies with severe movement disorder in mice expressing A53T human α-synuclein. Neuron *34*, 521–533.

Giasson, B.I., Forman, M.S., Higuchi, M., Golbe, L.I., Graves, C.L., Kotzbauer, P.T., Trojanowski, J.Q., and Lee, V.M.-Y. (2003). Initiation and synergistic fibrillization of tau and α-synuclein. Science *300*, 636–640.

Gilman, S., Low, P.A., Quinn, N., Albanese, A., Ben-Shlomo, Y., Fowler, C.J., Kaufmann, H., Klockgether, T., Lang, A.E., Lantos, P.L., et al. (1999). Consensus statement on the diagnosis of multiple system atrophy. J. Neurol. Sci. *163*, 94–98.

Goldstein, M.E., Cooper, H.S., Bruce, J., Carden, M.J., Lee, V.M.-Y., and Schlaepfer, W.W. (1987). Phosphorylation of neurofilament proteins and chromatolysis following transection of rat sciatic nerve. J. Neurosci. *7*, 1586–1594.

Graham, J.G., and Oppenheimer, D.R. (1969). Orthostatic hypotension and nicotine sensitivity in a case of multiple system atrophy. J. Neurol. Neurosurg. Psychiatry *32*, 28–34.

Gravel, M., DiPolo, A., Velera, P.B., and Braun, P.E. (1998). Four-kilobase sequence of the mouse CNP gene directs spatial and temporal expression of lacZ in transgenic mice. J. Neurosci. Res. *53*, 393–404.

Griffiths, I., Klugmann, M., Anderson, T., Yool, D., Thomson, C., Schwab, M.H., Schneider, A., Zimmermann, F., McCulloch, M., Nadon, N., and Nave, K.-A. (1998). Axonal swellings and degeneration in mice lacking the major proteolipid of myelin. Science *280*, 1610–1613.

Hedreen, J.C., and Koliatsos, V.E. (1994). Phosphorylated neurofilaments in neuronal perikarya and dendrites in human brain following axonal damage. J. Neuropathol. Exp. Neurol. *53*, 663–671.

Higuchi, M., Ishihara, T., Zhang, B., Hong, M., Andreadis, A., Trojanowski, J.Q., and Lee, V.M.-Y. (2002). Transgenic mouse model of tauopathies with glial pathology and nervous system degeneration. Neuron *35*, 433–446.

Iwai, A., Masliah, E., Yoshimoto, M., Ge, N., Flanagan, L., Rohan de Silva, H.A., Kittel, A., and Saitoh, T. (1995). The precursor protein of non-Aβ component of Alzheimer's disease amyloid is a presynaptic protein of the central nervous system. Neuron *14*, 467–475.

Jakes, R., Spillantini, M.G., and Goedert, M. (1994). Identification of two distinct synucleins from human brain. FEBS Lett. *345*, 27–32.

Jakes, R., Crowther, R.A., Lee, V.M.-Y., Trojanowski, J.Q., Iwatsubo, T., and Goedert, M. (1999). Epitope mapping of LB509, a monoclonal antibody directed against human α-synuclein. Neurosci. Lett. *269*, 13–16.

Kahle, P.J., Neumann, M., Ozmen, L., Muller, V., Jacobsen, H., Schindzielorz, A., Okochi, M., Leimer, U., Putten, H., Probst, A., et al. (2000). Subcellular localization of wild-type and Parkinson's disease-associated mutant α-synuclein in human and transgenic mouse brain. J. Neurosci. *20*, 6365–6373.

Kahle, P.J., Neumann, M., Ozmen, L., Muller, V., Jacobsen, H., Spooren, W., Fuss, B., Mallon, B., Macklin, W.B., Fujiwara, H., et al. (2002). Hyperphosphorylation and insolubility of α-synuclein in transgenic mouse oligodendrocytes. EMBO Rep. *3*, 583–588.

Klosen, P., Anderton, B.H., Brion, J.-P., and van den Bosch de Aguilar, P. (1990). Perikaryal neurofilament phosphorylation in axotomized and 6-OH-dopamine-lesioned CNS neurons. Brain Res. *526*, 259–269.

Masliah, E., Rockenstein, E., Veinbergs, I., Mallory, M., Hashimoto, M., Takeda, A., Sagara, Y., Sisk, A., and Mucke, L. (2000). Dopaminergic loss and inclusion body formation in α-synuclein mice: Implications for neurodegenerative disorders. Science *287*, 1265–1269.

Matsuo, A., Akiguchi, I., Lee, G.C., McGeer, E.G., and Kimura, J. (1998). Myelin degeneration in multiple system atrophy detected by unique antibodies. Am. J. Pathol. *153*, 735–744.

McGeer, P.L., Kawamata, T., Walker, D.G., Akiyama, H., Tooyama, H., and McGeer, E.G. (1993). Microglia in degenerative neurological disease. Glia *7*, 84–92.

Nakazato, Y., Yamazaki, H., Hirato, J., Ishida, Y., and Yamaguchi, H. (1990). Oligodendroglia microtubular tangles in olivopontocerebellar atrophy. J. Neuropathol. Exp. Neurol. *49*, 521–530.

Papp, M.I., and Lantos, P.L. (1994). The distribution of oligodendroglial inclusions in multiple system atrophy and its relevance to clinical symptomatology. Brain *117*, 235–243.

Papp, M.I., Kahn, J.E., and Lantos, P.L. (1989). Glial cytoplasmic inclusions in the CNS of patients with multiple system atrophy (striatonigral degeneration, olivopontocerebellar atrophy and Shy-Drager syndrome). J. Neurol. Sci. *94*, 79–100.

Perlmutter, L.S., Barron, E., and Chui, H.C. (1990). Morphologic association between microglia and senile plaque amyloid in Alzheimer's disease. Neurosci. Lett. *119*, 32–36.

Peters, A., Palay, S.L., and Webster, H.D. (1991). Morphologic association between microglia and senile plaque amyloid in Alzheimer's disease. In The Fine Structure of the Nervous System (New York: Oxford University Press), pp. 298–302.

Raeber, A.J., Race, R.E., Brandner, S., Priola, S.A., Sailer, A., Bessen, R.A., Mucke, L., Manson, J., Aguzzi, A., Oldstone, M.B.A., et al. (1997). Astrocyte-specific expression of hamster prion protein (PrP) renders PrP knockout mice susceptible to hamster scrapie. EMBO J. *16*, 6057–6065.

Rodriguez, E.M., Yulis, R., Peruzzo, B., Alvial, G., and Andrade, R.

(1984). Standardization of various applications of methacrylate embedding and silver methylamine for light and electron microscopy immunocytochemistry. Histochemistry *81*, 253–263.

Schmidt, M.L., Murray, J., Lee, V.M.-Y., Hill, W.D., Wertkin, A., and Trojanowski, J.Q. (1991). Epitope map of neurofilament protein domains in cortical and peripheral nervous system Lewy bodies. Am. J. Pathol. *139*, 53–65.

Spillantini, M.G., and Goedert, M. (2000). The α-synucleinopathies: Parkinson's disease, dementia with Lewy bodies, and multiple system atrophy. Ann. N Y Acad. Sci. *920*, 16–27.

Spillantini, M.G., Crowther, R.A., Jakes, R., Cairns, N.J., Lantos, P.L., and Goedert, M. (1998). Filamentous α-synuclein inclusions link multiple system atrophy with Parkinson's disease and dementia with Lewy bodies. Neurosci. Lett. *251*, 205–208.

Sternberger, N.H., Sternberger, L.A., and Ulrich, J. (1985). Aberrant neurofilament phosphorylation in Alzheimer disease. Proc. Natl. Acad. Sci. USA *82*, 4274–4276.

Trapp, B.D., Peterson, J., Ransohoff, R.M., Rudick, R., Mork, S., and Bo, L. (1998). Axonal transection in the lesions of multiple sclerosis. N. Engl. J. Med. *338*, 278–285.

Trojanowski, J.Q., Schuck, T., Schmidt, L.S., and Lee, V.M.-Y. (1989). Distribution of tau protein in the normal human central and peripheral nervous system. J. Histochem. Cytochem. *37*, 209–215.

Tu, P.H., Galvin, J.E., Baba, M., Giasson, B., Tomita, T., Leight, S., Nakajo, S., Iwatsubo, T., Trojanowski, J.Q., and Lee, V.M.-Y. (1998). Glial cytoplasmic inclusions in white matter oligodendrocytes of multiple system atrophy brains contain insoluble α-synuclein. Ann. Neurol. *44*, 415–422.

Vogelsberg-Ragaglia, V., Schuck, T., Trojanowski, J.Q., and Lee, V.M.-Y. (2001). PP2A mRNA expression is quantitatively decreased in Alzheimer's disease hippocampus. Exp. Neurol. *168*, 402–412.

Yamada, T., and McGeer, P.L. (1990). Oligodendroglial microtubular masses: an abnormality observed in some human neurodegenerative diseases. Neurosci. Lett. *120*, 163–166.